

IEM-FT-191/99
CERN-TH/99-103
IFT-UAM/CSIC-99-15
hep-ph/9904395

Naturalness of nearly degenerate neutrinos

J.A. Casas^{1,2*}, J.R. Espinosa^{2†}, A. Ibarra^{1‡} and I. Navarro^{1§}

¹ Instituto de Estructura de la materia, CSIC

Serrano 123, 28006 Madrid

² Theory Division, CERN

CH-1211 Geneva 23, Switzerland.

Abstract

If neutrinos are to play a relevant cosmological role, they must be essentially degenerate. We study whether radiative corrections can or cannot be responsible for the small mass splittings, in agreement with all the available experimental data. We perform an exhaustive exploration of the bimaximal mixing scenario, finding that (i) the vacuum oscillations solution to the solar neutrino problem is always excluded; (ii) if the mass matrix is produced by a see-saw mechanism, there are large regions of the parameter space consistent with the large angle MSW solution, providing a natural origin for the $\Delta m_{sol}^2 \ll \Delta m_{atm}^2$ hierarchy; (iii) the bimaximal structure becomes then stable under radiative corrections. We also provide analytical expressions for the mass splittings and mixing angles and present a particularly simple see-saw ansatz consistent with all observations.

CERN-TH/99-103

April 1999

*E-mail: casas@mail.cern.ch

†E-mail: espinosa@mail.cern.ch

‡E-mail: alejandromakoki@iem.csic.es

§Email: ignacio@makoki.iem.csic.es

1 Introduction

Standard explanations of the observed atmospheric and solar neutrino anomalies [1] require neutrino oscillations between different species, which imply that neutrinos are massive, with mass-squared differences of at most 10^{-2} eV². On the other hand, if neutrinos are to play an essential role in the large scale structure of the universe, the sum of their masses must be a few eV, and therefore they must be almost degenerate. This scenario has recently attracted much attention [2]-[5]. In this paper we will analyze under which circumstances the “observed” mass differences arise naturally (or not), as a radiative effect, in agreement with all the available experimental data.

Let us briefly review the current relevant experimental constraints on neutrino masses and mixing angles. Observations of atmospheric neutrinos require $\nu_\mu - \nu_\tau$ oscillations driven by a mass splitting and a mixing angle in the range [6]

$$\begin{aligned} 5 \times 10^{-4} \text{ eV}^2 < \Delta m_{at}^2 < 10^{-2} \text{ eV}^2, \\ \sin^2 2\theta_{at} > 0.82. \end{aligned} \tag{1}$$

On the other hand, there are three main explanations of the solar neutrino flux deficits, requiring oscillations of electron neutrinos into other species. The associated mass splittings and mixing angles depend on the type of solution:

Small angle MSW (SAMSW) solution:

$$\begin{aligned} 3 \times 10^{-6} \text{ eV}^2 < \Delta m_{sol}^2 < 10^{-5} \text{ eV}^2, \\ 4 \times 10^{-3} < \sin^2 2\theta_{sol} < 1.3 \times 10^{-2}. \end{aligned} \tag{2}$$

Large angle MSW (LAMSW) solution:

$$\begin{aligned} 10^{-5} \text{ eV}^2 < \Delta m_{sol}^2 < 2 \times 10^{-4} \text{ eV}^2, \\ 0.5 < \sin^2 2\theta_{sol} < 1. \end{aligned} \tag{3}$$

Vacuum oscillations (VO) solution:

$$\begin{aligned} 5 \times 10^{-11} \text{ eV}^2 < \Delta m_{sol}^2 < 1.1 \times 10^{-10} \text{ eV}^2, \\ \sin^2 2\theta_{sol} > 0.67. \end{aligned} \tag{4}$$

Let us remark the hierarchy of mass splittings between the different species of neutrinos, $\Delta m_{sol}^2 \ll \Delta m_{at}^2$, which is apparent from eqs.(1, 2–4). This hierarchy should be reproduced by any natural explanation of those splittings.

As it has been shown in ref. [2] the small angle MSW solution is unphysical in a scenario of nearly degenerate neutrinos, so we are left with the LAMSW and VO possibilities.

An important point concerns the upper limit on $\sin^2 2\theta_{sol}$ in the LAMSW solution. According to ref.[4] the absolute limit $\sin^2 2\theta_{sol} = 1$ is forbidden at 99.8%, but with no indication about the tolerable upper limit. In this sense a conservative upper bound $\sin^2 2\theta_{sol} < 0.99$ can be adopted. However, recent combined analysis of data, including the day–night effect, indicate that even the $\sin^2 2\theta_{sol} = 1$ possibility is allowed at 99% for $2 \times 10^{-5} \text{ eV}^2 < \Delta m_{sol}^2 < 1.7 \times 10^{-4} \text{ eV}^2$ [7], although there may be problems to define the upper limit on $\sin^2 2\theta_{sol}$ in a precise sense [8]. For the moment we will not adopt an upper bound on $\sin^2 2\theta_{sol}$, but later on we will show the effect of such a bound on the results, which turns out to be dramatic.

Finally, the non-observation of neutrinoless double β -decay puts an upper bound on the ee element of the Majorana neutrino mass matrix, namely [9]

$$\mathcal{M}_{ee} < B = 0.2 \text{ eV}. \quad (5)$$

Concerning the cosmological relevance of neutrinos, as mentioned above, we will assume $\sum m_{\nu_i} = O(\text{eV})$. In particular, we will take $\sum m_{\nu_i} = 6 \text{ eV}$ as a typical possibility, although as we will see, the results do not depend essentially on the particular value. It should be mentioned here that Tritium β -decay experiments indicate $m_{\nu_i} < 2.5 \text{ eV}$ for any mass eigenstate with a significant ν_e component [10].

Using standard notation, we define the effective mass term for the three light (left-handed) neutrinos in the flavour basis as

$$\mathcal{L} = -\frac{1}{2}\nu^T \mathcal{M}_\nu \nu + \text{h.c.} \quad (6)$$

where \mathcal{M}_ν is the neutrino mass matrix. This is diagonalized in the usual way

$$\mathcal{M}_\nu = V^* D V^\dagger, \quad (7)$$

where V is a unitary ‘CKM’ matrix, relating the flavor eigenstates to the mass eigen-

states

$$\begin{pmatrix} \nu_e \\ \nu_\mu \\ \nu_\tau \end{pmatrix} = \begin{pmatrix} c_2 c_3 & c_2 s_3 & s_2 e^{-i\delta} \\ -c_1 s_3 - s_1 s_2 c_3 e^{i\delta} & c_1 c_3 - s_1 s_2 s_3 e^{i\delta} & s_1 c_2 \\ s_1 s_3 - c_1 s_2 c_3 e^{i\delta} & -s_1 c_3 - c_1 s_2 s_3 e^{i\delta} & c_1 c_2 \end{pmatrix} \begin{pmatrix} \nu_1 \\ \nu_2 \\ \nu_3 \end{pmatrix}, \quad (8)$$

where s_i and c_i denote $\sin \theta_i$ and $\cos \theta_i$ respectively. D may be written as

$$D = \begin{pmatrix} m_1 e^{i\phi} & 0 & 0 \\ 0 & m_2 e^{i\phi'} & 0 \\ 0 & 0 & m_3 \end{pmatrix}. \quad (9)$$

It should be mentioned here that, for a given mass matrix, the θ_i angles are not uniquely defined, unless one gives a criterion to order the mass eigenvectors ν_i in eq.(8) (e.g. $m_{\nu_1}^2 < m_{\nu_2}^2 < m_{\nu_3}^2$). Of course, the corresponding V matrices differ just in the ordering of the columns, and thus are physically equivalent.

In this notation, constraint (5) reads

$$\mathcal{M}_{ee} \equiv |m_{\nu_1} c_2^2 c_3^2 e^{i\phi} + m_{\nu_2} c_2^2 s_3^2 e^{i\phi'} + m_{\nu_3} s_2^2 e^{i2\delta}| < B. \quad (10)$$

As it has been put forward by Georgi and Glashow in ref. [2], a scenario of nearly degenerate neutrinos plausibly leads to $\theta_2 \simeq 0$. In that case, eq.(10), yields $\sin^2 2\theta_3 \geq 0.99$, which, as discussed above, might be in conflict with the LAMSW solution to the solar neutrino anomaly. However, according to some fits, θ_2 could be as large as 23° or even 45° [6]. Therefore, although small values of θ_2 are clearly preferred, in some cases a non-negligible contribution of $\sin^2 \theta_2$ in eq.(10) is enough to relax the above mentioned stringent bound on $\sin^2 2\theta_3$, and in fact we will see some examples of this feature later on. Our criterion throughout the paper will be to keep eq.(5) [or the complete eq.(10)] as the neutrinoless double β -decay constraint, without demanding any extra condition on θ_3, θ_2 . In any case, we will see that in all viable cases $\sin^2 2\theta_3 \geq 0.99$ and θ_2 is very small.

Let us now discuss the strategy we have followed to analyze if the required mass splittings and mixing angles can or cannot arise in a natural way through radiative corrections.

Following ref. [2] (some of their arguments have been discussed above), the scenario of nearly degenerate neutrinos should be close to a bimaximal mixing, which constrains

the texture of the mass matrix \mathcal{M}_ν to be [2,3]

$$\mathcal{M}_b = m_\nu \begin{pmatrix} 0 & \frac{1}{\sqrt{2}} & \frac{1}{\sqrt{2}} \\ \frac{1}{\sqrt{2}} & \frac{1}{2} & -\frac{1}{2} \\ \frac{1}{\sqrt{2}} & -\frac{1}{2} & \frac{1}{2} \end{pmatrix}, \quad (11)$$

where m_ν is a general mass scale. \mathcal{M}_b can be diagonalized by a V matrix

$$V_b = \begin{pmatrix} \frac{-1}{\sqrt{2}} & \frac{1}{\sqrt{2}} & 0 \\ \frac{1}{2} & \frac{1}{2} & \frac{-1}{\sqrt{2}} \\ \frac{1}{2} & \frac{1}{2} & \frac{1}{\sqrt{2}} \end{pmatrix}, \quad (12)$$

leading to exactly degenerate neutrinos: $D = m_\nu \text{diag}(-1, 1, 1)$ and $\theta_2 = 0$, $\sin^2 2\theta_3 = \sin^2 2\theta_1 = 1$. Let us remind that in this scenario only the LAMSW and VO solutions to the solar anomaly are acceptable.

The nice aspect of \mathcal{M}_b suggests that it could be generated at some scale by interactions obeying appropriate continuous or discrete symmetries. This is an interesting issue [11], which we will not address in this paper. On the other hand, in order to be realistic, the effective matrix \mathcal{M}_ν at low energy should be certainly close to \mathcal{M}_b , but it must be *slightly* different in order to account for the mass splittings given in eqs.(1,3,4). The main goal of this paper is to explore whether the appropriate splittings (and mixing angles) can be generated or not through radiative corrections; more precisely, through the running of the renormalization group equations (RGEs) between the scale at which \mathcal{M}_ν is generated and low energy. The output of this analysis can be of three types:

- i)* All the mass splittings and mixing angles obtained from the RG running are in agreement with all experimental limits and constraints.
- ii)* Some (or all) mass splittings are much larger than the acceptable ranges.
- iii)* Some (or all) mass splittings are smaller than the acceptable ranges, and the rest is within.

Case (*i*) is obviously fine. Case (*ii*) is disastrous. The only way-out would be an extremely artificial fine-tuning between the initial form of \mathcal{M}_ν and the effect of

the RG running. Hence we consider this possibility unacceptable. Finally, case *(iii)* is not fine, in the sense that the RGEs fail to explain the required modifications of \mathcal{M}_ν . However, it leaves the door open to the possibility that other (not specified) effects could be responsible for them. In that case, the RGE would not spoil a fine pre-existing structure. Consequently, we consider this possibility as undecidable. We will see along the paper different scenarios corresponding to the three possibilities.

Concerning the mixing angles, it is worth stressing that, due to the two degenerate eigenvalues of \mathcal{M}_b , V_b is not uniquely defined (V_b times any rotation on the plane of degenerate eigenvalues is equally fine). Hence, once the ambiguity is removed thanks to the small splittings coming from the RG running, the mixing angles may be very different from the desired ones. However, if those cases correspond to the previous *(iii)* possibility, they are still of the “undecidable” type with respect to the mixing angles, since the modifications of \mathcal{M} (of non-specified origin) needed to reproduce the correct mass splittings will also change dramatically the mixing angles.

In section 2, we first examine the general case in which the neutrino masses arise from an effective operator, remnant from new physics entering at a scale Λ . In this framework, we take a low energy point of view, assuming a bimaximal-mixing mass structure at the scale Λ as an initial condition. In this section we do not consider possible perturbations of that initial condition coming from high-energy effects. We find this case to be of the undecidable type [possibility *(iii)* above], except for the VO solution, which is excluded.

In section 3 we go one step further and consider in detail a particularly well motivated example of the previous case: the see-saw scenario. We include now the high energy effects of the new degrees of freedom above the scale Λ (identified with the Majorana mass). We find regions of parameter space where the neutrino spectrum and mixing angles fall naturally in the pattern required to explain solar (LAMSW solution) and atmospheric neutrino anomalies, which we find remarkable. We complement the numerical results with compact analytical formulas which give a good description of them, and allow to understand the pattern of mass splittings and mixing angles obtained. We also present a plausible texture for the neutrino Yukawa couplings leading to a good fit of the oscillation data. Finally we draw some conclusions.

2 \mathcal{M}_ν as an effective operator

In this section we consider the simplest possibility that the Majorana mass matrix for the left-handed neutrinos, \mathcal{M}_ν , is generated at some high energy scale, Λ , by some unspecified mechanism (we allow Λ to vary from M_p to M_Z). Assuming that the only light fields below Λ are the Standard Model (SM) ones, the lowest dimension operator producing a mass term of this kind is uniquely given by [13]

$$-\frac{1}{4}\kappa\nu^T\nu HH + \text{h.c.} \quad (13)$$

where κ is a matricial coupling and H is the ordinary (neutral) Higgs. Obviously, $\mathcal{M}_\nu = \frac{1}{2}\kappa\langle H\rangle^2$. The effective coupling κ runs with the scale below Λ , with a RGE given by [14]

$$16\pi^2\frac{d\kappa}{dt} = \left[-3g_2^2 + 2\lambda + 6Y_t^2 + 2\text{Tr}\mathbf{Y}_e^\dagger\mathbf{Y}_e\right]\kappa - \frac{1}{2}\left[\kappa\mathbf{Y}_e^\dagger\mathbf{Y}_e + (\mathbf{Y}_e^\dagger\mathbf{Y}_e)^T\kappa\right], \quad (14)$$

where $t = \log\mu$, and $g_2, \lambda, Y_t, \mathbf{Y}_e$ are the $SU(2)$ gauge coupling, the quartic Higgs coupling, the top Yukawa coupling and the matrix of Yukawa couplings for the charged leptons, respectively. Let us note that the RGE depends on λ , and thus on the value of the Higgs mass, m_H . We have taken $m_H = 150$ GeV throughout the paper, but in any case the dependence is very small (it slightly affects the overall neutrino mass scale but not the relative splittings).

In the scenario in which we are interested (almost degenerate neutrinos), the simplest assumption about the form of κ is that the interactions responsible for it produce the bimaximal mixing texture of eq.(11). Hence

$$\mathcal{M}_\nu(\Lambda) = \frac{1}{2}\kappa(\Lambda)\langle H\rangle^2 = \mathcal{M}_b. \quad (15)$$

Clearly, the last term of the RGE (14) will slightly perturb the initial form of \mathcal{M}_ν , so we expect at low energy small mass splittings, and mixing angles different from the bimaximal case.

In order to gain intuition on the final (low energy) form of \mathcal{M}_ν , and the corresponding mass splittings and mixing angles, it is convenient to neglect for a while all the charged lepton Yukawa couplings but Y_τ . Then κ maintains its form along the running,

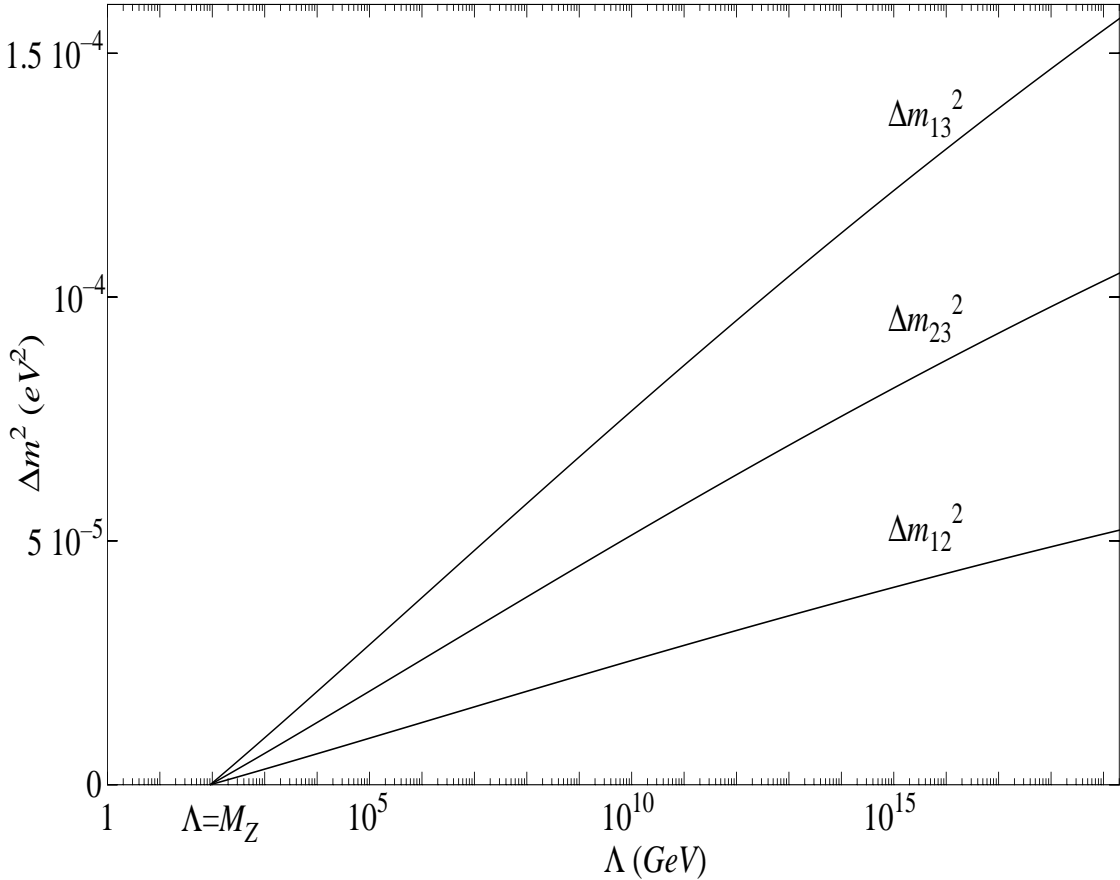


Figure 1: Dependence of neutrino mass splittings at low energy (Δm_{ij}^2 in eV^2) with the cut-off scale Λ (GeV).

except for the third row and column:

$$\mathcal{M}_\nu(\mu_0) \propto \begin{pmatrix} 0 & \frac{1}{\sqrt{2}} & \frac{1}{\sqrt{2}}(1+\epsilon) \\ \frac{1}{\sqrt{2}} & \frac{1}{2} & -\frac{1}{2}(1+\epsilon) \\ \frac{1}{\sqrt{2}}(1+\epsilon) & -\frac{1}{2}(1+\epsilon) & \frac{1}{2}(1+2\epsilon) \end{pmatrix} \quad (16)$$

where μ_0 is the low-energy scale, which can be identified with M_Z and ϵ has positive sign. Therefore, the mass eigenvalues are proportional to $-1 - \epsilon/2$, 1 , $1 + 3\epsilon/2$, and the corresponding splittings (adopting the convention $m_{\nu_1}^2 < m_{\nu_2}^2 < m_{\nu_3}^2$) are

$$\Delta m_{12}^2 = \frac{1}{2}\Delta m_{23}^2 = \frac{1}{3}\Delta m_{13}^2 \simeq m_\nu^2 \epsilon \quad (17)$$

Clearly, these mass splittings are incompatible with the required hierarchy $\Delta m_{sol}^2 \ll \Delta m_{at}^2$, of eqs.(1, 3, 4). We will discuss the size of these splittings shortly. Equation

(16) is also useful to get an approximate form of the V matrix responsible for the diagonalization of \mathcal{M}_ν

$$V \simeq \begin{pmatrix} -\frac{1}{\sqrt{2}} & \frac{1}{\sqrt{3}} & \frac{1}{\sqrt{6}} \\ \frac{1}{2} & \sqrt{\frac{2}{3}} & -\frac{1}{2\sqrt{3}} \\ \frac{1}{2} & 0 & \frac{\sqrt{3}}{2} \end{pmatrix}, \quad (18)$$

which leads to mixing angles

$$\sin^2 2\theta_1 = \frac{9}{25}, \quad \sin^2 2\theta_2 = \frac{5}{9}, \quad \sin^2 2\theta_3 = \frac{24}{25}. \quad (19)$$

Clearly, these values are far away from the bimaximal mixing ones. In consequence, they are not acceptable.

The previous failures of the scenario considered in this section in order to reproduce the mass splittings and the mixing angles indicate that we are in one of the two possibilities (ii) or (iii) discussed in the Introduction. To go further, we need a numerical evaluation of the mass splittings, and thus of ϵ . Solving the RGE (14) at lowest order, we simply find

$$\epsilon = \frac{Y_\tau^2}{32\pi^2} \log \frac{\Lambda}{\mu_0}. \quad (20)$$

So, from eq.(17) the mass splittings are typically of order 10^{-5} eV^2 . This is confirmed by the complete numerical evaluation of the RGE, which gives the mass splittings shown in Fig.1.

The first conclusion is that for any Λ (even very close to μ_0) the mass splittings are much larger than those required for the VO solution to the solar neutrino problem, $\Delta m_{sol}^2 \sim 10^{-10} \text{ eV}^2$. Therefore, the effect of the RGE for this scenario is disastrous in the sense discussed in the Introduction for the possibility (ii). In consequence the VO solution to the solar neutrino problem is excluded.

For the LAMSW solution to the solar neutrino problem, things are a bit different. Clearly, the mass splittings obtained from the RGE analysis are within or below the required range, eq.(3), for almost any value of the cut-off scale Λ . In addition, the mass splittings are clearly below the atmospheric range, eq.(1). Therefore, we are in the case (ii) discussed in the Introduction: The radiative corrections fail to provide an origin to the required mass splittings and mixing angles, but they will not destroy a

suitable initial modification (from unspecified origin) of \mathcal{M}_ν at the Λ scale. It is anyway remarkable that the radiative corrections place Δm^2 just in the right magnitude for the LAMSW solution.

In the next section we will discuss a natural source for the initial modification of \mathcal{M}_ν , which leads naturally to completely satisfactory (atmospheric plus LAMSW) scenarios.

3 \mathcal{M}_ν from the see-saw mechanism

A natural way of obtaining small neutrino masses is the so-called see-saw mechanism [15] in which the particle content of the Standard Model is enlarged by one additional neutrino field (not charged under the SM group) per generation, $\nu_{\alpha,R}$ ($\alpha = e, \mu, \tau$). The Lagrangian reads

$$\mathcal{L} = -\bar{\nu}_R m_D \nu + \frac{1}{2} \bar{\nu}_R \mathcal{M} \bar{\nu}_R^T + \text{h.c.} \quad (21)$$

Here m_D is a 3×3 Dirac mass matrix with magnitude determined by the electroweak breaking scale, $m_D = \mathbf{Y}_\nu \langle H \rangle$, where \mathbf{Y}_ν is the matrix of neutrino Yukawa couplings and $\langle H \rangle = 246/\sqrt{2}$ GeV; and \mathcal{M} is a 3×3 Majorana mass matrix which does not break the SM gauge symmetry. Thus, the overall scale of \mathcal{M} , which we will denote by M , can be naturally many orders of magnitude higher than the electroweak scale. In that case, the low-energy effective theory, after integrating out the heavy $\nu_{\alpha,R}$ fields [whose masses are $O(M)$], is just the SM with left-handed neutrino masses given by

$$\mathcal{M}_\nu = m_D^T \mathcal{M}^{-1} m_D = \mathbf{Y}_\nu^T \mathcal{M}^{-1} \mathbf{Y}_\nu \langle H \rangle^2, \quad (22)$$

suppressed with respect to the typical fermion masses by the inverse power of the large scale M .

In this appealing framework, the degeneracy in neutrino masses can come about as a result of some symmetry (at some high energy, e.g. M_p) in the textures of \mathcal{M} and \mathbf{Y}_ν such that $\mathcal{M}_\nu(M_p) = \mathcal{M}_b$. Starting from this very symmetric condition at M_p we make contact with the low energy neutrino mass matrix using the renormalization group. First we run \mathcal{M} and \mathbf{Y}_ν from M_p down to M , where the right-handed neutrinos are decoupled. Below that scale and all the way down to low energy we run \mathcal{M}_ν as an effective operator, in the same way as in the previous section. We can also think

of the first stage of running between M_p and M as the high energy effects providing an starting form of \mathcal{M} for the second stage of running, i.e. the only one considered in the previous section (the role of Λ is played by M). This form, being slightly different from \mathcal{M}_b , may rescue the previous “undecidable” cases.

In pursuing this idea, it is natural to assume [12] that the structure leading to the relation $\mathcal{M}_\nu(M_p) = \mathcal{M}_b$ occurs either in the Dirac matrix m_D [while the Majorana matrix \mathcal{M} is simply diagonal with equal eigenvalues (up to a sign)²] or in the Majorana matrix [with a simple diagonal Dirac matrix (again with eigenvalues equal up to a sign)]. We cannot expect a conspiracy between both matrices (which come from totally different physics) leading to $\mathcal{M}_\nu(M_p) = \mathcal{M}_b$.

3.1 Textures of \mathcal{M} and \mathbf{Y}_ν leading to bimaximal mixing

In the analysis of what structures for \mathcal{M} or \mathbf{Y}_ν lead to $\mathcal{M}_\nu(M_p) = \mathcal{M}_b$ for simplicity we only consider real matrices (thus avoiding potential problems with CP violation).

If we assume that \mathbf{Y}_ν is proportional to the identity and all the structure arises from the Majorana mass matrix, then we simply need to impose $\mathcal{M}(M_p) \propto \mathcal{M}_b$ (note that $\mathcal{M}_b^{-1} \propto \mathcal{M}_b$). The alternative case is less trivial but equally simple. If \mathcal{M} is of the form³

$$\mathcal{M} = M \begin{pmatrix} -1 & 0 & 0 \\ 0 & 1 & 0 \\ 0 & 0 & 1 \end{pmatrix}, \quad (23)$$

then it is easy to see that the most general form of \mathbf{Y}_ν satisfying $\mathbf{Y}_\nu^T M^{-1} \mathbf{Y}_\nu \propto \mathcal{M}_b$ is

$$\mathbf{Y}_\nu = Y_\nu B V_b^T. \quad (24)$$

Here Y_ν is the overall magnitude of \mathbf{Y}_ν and B is a combination of two ‘boosts’

$$B = \begin{pmatrix} \cosh a & \sinh a & 0 \\ \sinh a & \cosh a & 0 \\ 0 & 0 & 1 \end{pmatrix} \begin{pmatrix} \cosh b & 0 & \sinh b \\ 0 & 1 & 0 \\ \sinh b & 0 & \cosh b \end{pmatrix}, \quad (25)$$

with two free parameters a, b . Actually, one could also take $\mathbf{Y}_\nu = Y_\nu R B V_b^T$, where R is a rotation in the (μ, τ) plane, but such rotations can be absorbed into a change of the

²Actually, the condition we are imposing is that the eigenvalues are equal (up to a sign). A suitable transformation will diagonalize \mathcal{M} to the form we assume.

³If \mathcal{M} is taken proportional to the identity, the Yukawa matrix \mathbf{Y}_ν must be chosen complex. Our choice of \mathcal{M} avoids that complication and is physically equivalent.

$(\nu_R)_\alpha$ basis, $\nu_R \rightarrow R\nu_R$, with no modification in \mathcal{M} and thus give physically equivalent results.

Let us notice that the former case, where all the structure is in the \mathcal{M} matrix, is equivalent to the latter case (all the structure in \mathbf{Y}_ν) if we set $a = b = 0$. To see this, note that a redefinition of the ν_R fields as $\nu_R \rightarrow V_b\nu_R$, would leave $\mathcal{M} \propto \text{diag}(-1, 1, 1)$ and $\mathbf{Y}_\nu = Y_\nu V_b^T$. In consequence, it is enough to study the case where all the structure is in \mathbf{Y}_ν , given by eq.(24).

3.2 Running \mathcal{M}_ν from M_p to low energy

From M_p to M the evolution of the relevant matrices is governed by the following renormalization group equations:

$$\frac{d\mathbf{Y}_\nu}{dt} = -\frac{1}{16\pi^2}\mathbf{Y}_\nu \left[\left(\frac{9}{4}g_2^2 + \frac{3}{4}g_1^2 - \mathbb{T} \right) \mathbf{I}_3 - \frac{3}{2}(\mathbf{Y}_\nu^\dagger\mathbf{Y}_\nu + \mathbf{Y}_e^\dagger\mathbf{Y}_e) \right], \quad (26)$$

$$\frac{d\mathbf{Y}_e}{dt} = -\frac{1}{16\pi^2}\mathbf{Y}_e \left[\left(\frac{9}{4}g_2^2 + \frac{15}{4}g_1^2 - \mathbb{T} \right) \mathbf{I}_3 + \frac{3}{2}(\mathbf{Y}_\nu^\dagger\mathbf{Y}_\nu + \mathbf{Y}_e^\dagger\mathbf{Y}_e) \right], \quad (27)$$

where

$$\mathbb{T} = \text{Tr}(3\mathbf{Y}_U^\dagger\mathbf{Y}_U + 3\mathbf{Y}_D^\dagger\mathbf{Y}_D + \mathbf{Y}_\nu^\dagger\mathbf{Y}_\nu + \mathbf{Y}_e^\dagger\mathbf{Y}_e), \quad (28)$$

and

$$\frac{d\mathcal{M}}{dt} = \frac{1}{16\pi^2} \left[\mathcal{M}(\mathbf{Y}_\nu\mathbf{Y}_\nu^\dagger)^T + \mathbf{Y}_\nu\mathbf{Y}_\nu^\dagger\mathcal{M} \right]. \quad (29)$$

Here g_2 and g_1 are the $SU(2)_L$ and $U(1)_Y$ gauge coupling constants, and $\mathbf{Y}_{U,D,e}$ are the Yukawa matrices for up quarks, down quarks and charged leptons.

At M , ν_R decouple, and \mathbf{Y}_e must be diagonalized to redefine the flavour basis of leptons [note that the last term in (27) produces non-diagonal contributions to \mathbf{Y}_e] affecting the form of the \mathbf{Y}_ν matrix. Then the effective mass matrix for the light neutrinos is $\mathcal{M}_\nu \simeq \mathbf{Y}_\nu^T \mathcal{M}^{-1} \mathbf{Y}_\nu \langle H \rangle^2$.

From M to M_Z , the effective mass matrix \mathcal{M}_ν is run down in energy exactly as described in section 2. The renormalization group equations are integrated with the following boundary conditions: \mathcal{M} and \mathbf{Y}_ν are chosen at M_p so as to satisfy

$$\mathcal{M}_\nu(M_p) = \mathcal{M}_b, \quad (30)$$

with the overall magnitude of \mathbf{Y}_ν fixed, for a given value of the Majorana mass M , by the requirement $m_\nu \sim O(\text{eV})$. The boundary conditions for the other Yukawa couplings are fixed at the low energy side to give the observed fermion masses. The free parameters are therefore M, a and b .

3.3 Limits on the parameter space

We discuss here the limits on the parameter space of our study, which is expanded by M, a and b .

The parameters a and b , which define the texture of the \mathbf{Y}_ν matrix through eqs.(24, 25), can be in principle any real numbers. However, it is apparent from eqs.(24, 25) that if a or b are large, the entries of \mathbf{Y}_ν are extremely fine-tuned. Notice that the relative difference between $\cosh a$ and $\sinh a$ factors is $\sim 2e^{-2|a|}$ (and the analogue for $\cosh b$ and $\sinh b$). Therefore, the \mathbf{Y}_ν matrix is fine-tuned as $\sim 2e^{-2(|a|+|b|)}$ parts in one. In particular, if $|a|$ or $|b|$ are > 1.5 the matrix elements are fine-tuned at least in a 10%. In consequence, we will demand

$$|a|, |b| \leq 1.5. \quad (31)$$

Let us remark that the previous limits are based on a criterion of naturality for the \mathbf{Y}_ν matrix. However, let us mention that if we relax these limits, the final results (to be presented in the next subsection) are basically unchanged, since the allowed regions for a, b remain in the “natural” region (31) in most of the cases.

Concerning the remaining parameter, M , there is an upper bound on it coming from the fact that for large values of M , the neutrino Yukawa couplings, \mathbf{Y}_ν , develop Landau poles below M_p , spoiling the perturbativity of the theory [16]. This occurs for $M(M_p) \sim 4.3 \times 10^{13}$ GeV. Actually, there is an additional effect, namely the closing of the allowed Higgs window, which occurs approximately for the same value of $M(M_p)$. Consequently, this sets the upper bound on M . It is interesting to note that this effect also restricts the values of a, b : for a given M , the larger a, b , the larger the entries of \mathbf{Y}_ν , and thus the lower the scale at which the Landau pole appears. In general, this restriction on a, b is less severe than eq.(31).

Regarding the lower bound on M , there is no physical criterion for it, as the actual origin of the right-handed Majorana matrix is unknown. Since M can be written in terms of m_ν and \mathbf{Y}_ν (roughly speaking $M \simeq Y_\nu^2 \langle H \rangle^2 / m_\nu$), we can adopt the sensible

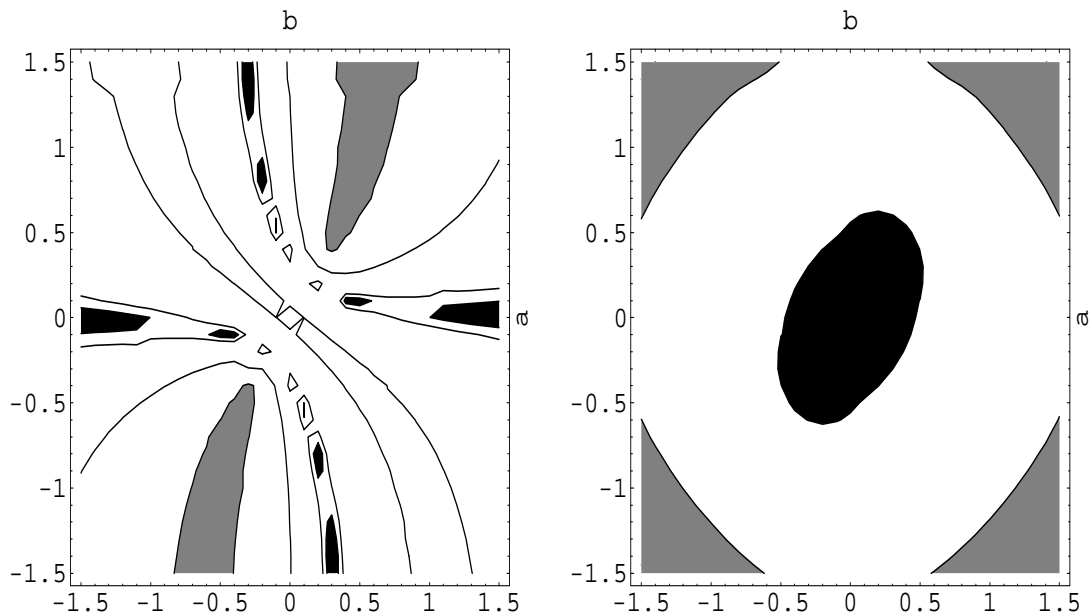


Figure 2: Left plot: contours of $\Delta m_{12}^2/eV^2$ in the (b, a) plane from less than 10^{-5} (black area), through 2×10^{-5} and 10^{-4} (lines) to more than 2×10^{-4} (grey). Right plot: same for $\Delta m_{23}^2/eV^2$, from 5×10^{-4} (black) to 10^{-2} (grey). The Majorana mass is 8×10^9 GeV.

criterion that Y_ν is at least as large as the smallest Yukawa coupling so far known, i.e. the electron one. This precisely corresponds to $M \sim 100$ GeV, below which is unphysical to descend. In consequence, our limits for M are

$$10^2 \text{GeV} \lesssim M \lesssim 4.3 \times 10^{13} \text{GeV}. \quad (32)$$

On the other hand, as we will see in the next subsection, there are no physically viable scenarios unless

$$M \gtrsim 10^8 \text{GeV}, \quad (33)$$

which sets an operating lower limit on M .

3.4 Results

Figures 2 to 6 present our results for the mass splittings and mixing angles at low energy, after numerical integration of the RGEs from M_p to low energy as described in subsection 3.2 (we follow the convention $m_{\nu_1}^2 < m_{\nu_2}^2 < m_{\nu_3}^2$ in all the figures). We have

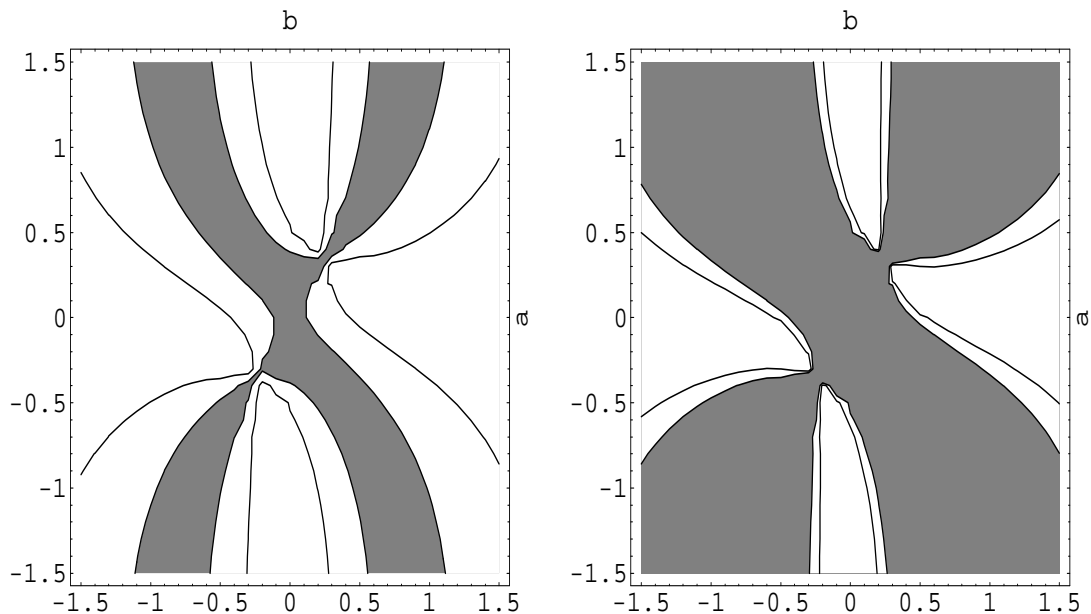


Figure 3: Left plot: Contours of $\sin^2 2\theta_2$ in the (b, a) plane. The grey area marks the $\sin^2 2\theta_2 > 0.52$ region. The line singled-out corresponds to $\sin^2 2\theta_2 = 0.19$. Right plot: Contours of $\sin^2 2\theta_1$ in the (b, a) plane. In the grey area $\sin^2 2\theta_1$ is smaller than 0.82, and the line corresponds to $\sin^2 2\theta_1 = 0.9$. The Majorana mass is 8×10^9 GeV.

chosen $M = 8 \times 10^9$ GeV as a typical example; the dependence of the results with M is discussed later on.

Figure 2, left plot, shows contour lines of constant Δm_{12}^2 (the squared mass difference between the lightest neutrinos) in the plane (b, a) . The black (grey) region is excluded because there $\Delta m_{12}^2 < 10^{-5} \text{ eV}^2$ ($\Delta m_{12}^2 > 2 \times 10^{-4} \text{ eV}^2$), which is too small (large) to account for the oscillations of solar neutrinos (LAMSW solution). The white area is thus the allowed region. The lines in it correspond to $\Delta m_{12}^2 = 10^{-4} \text{ eV}^2$ and $2 \times 10^{-5} \text{ eV}^2$.

Figure 2, right plot, gives contour lines of constant Δm_{23}^2 . The black (grey) region is excluded because there $\Delta m_{23}^2 < 5 \times 10^{-4} \text{ eV}^2$ ($\Delta m_{23}^2 > 10^{-2} \text{ eV}^2$), which is too small (large) to account for the oscillations of atmospheric neutrinos. Again, the white area is allowed. We do not plot Δm_{13}^2 because it can always be inferred from Δm_{23}^2 and Δm_{12}^2 . Moreover, in the interesting case, $\Delta m_{12}^2 \ll \Delta m_{23}^2$, one has $\Delta m_{13}^2 \simeq \Delta m_{23}^2$.

The intersection of the white areas in both plots is non-zero and would give the

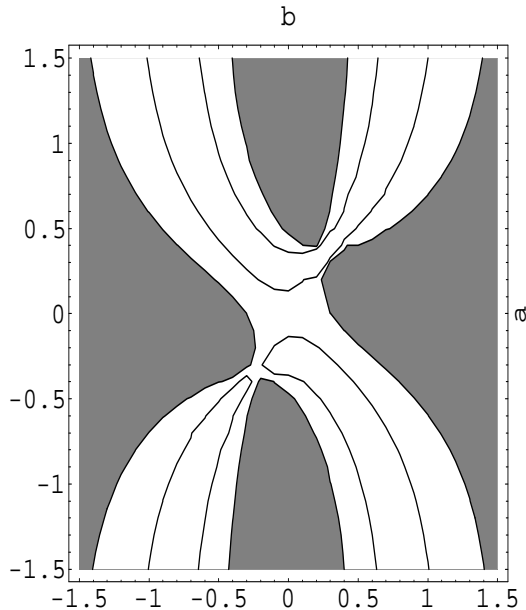


Figure 4: Same as figure 3 for $\sin^2 2\theta_3$. The grey area corresponds to values above 0.99. The curve gives $\sin^2 2\theta_3 = 0.95$.

allowed area concerning mass splittings. It is always the case that the area surrounding the origin is excluded. There, the mass differences are always of the same order, and follow the same pattern discussed in subsection 2 ($\Delta m_{23}^2 = 2\Delta m_{12}^2$). In any case we conclude that, away from the origin, there is a non negligible region of parameter space where it is natural to have $\Delta m_{23}^2 \gg \Delta m_{12}^2$ and in accordance with the values required to explain the solar and atmospheric neutrino anomalies. In the following subsection we explain the origin of this hierarchy of mass differences.

Next, we need to ensure that the mixing angles are the correct ones to give a good fit to atmospheric and solar neutrino data (as summarized by the ranges given in the Introduction). Figure 3, left plot, gives contours of constant $\sin^2 2\theta_2$ (one of the mixing angles relevant for atmospheric neutrino oscillations). The grey (white) area has $\sin^2 2\theta_2$ larger (smaller) than 0.52 and is disfavored (favored) by the data. However, as explained in the Introduction, we do not impose tight constraints on the value of this mixing angle. The line singled-out corresponds to $\sin^2 2\theta_2 = 0.19$ (preferred value from the fit of the first ref. in [6]).

Figure 3, right plot, shows contours of constant $\sin^2 2\theta_1$ (the other mixing angle rel-

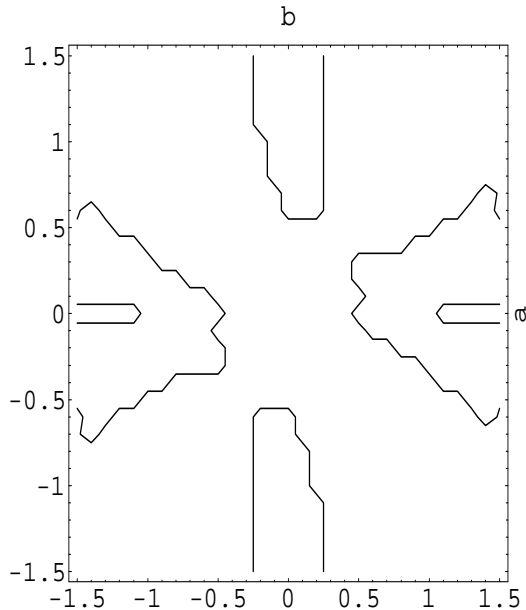


Figure 5: Region (disconnected parts) in the (b, a) parameter space for $M = 8 \times 10^9$ GeV where all mass splittings and mixing angles satisfy experimental constraints. (See text for qualifications).

evant for atmospheric neutrinos). The grey (white) area corresponds to $\sin^2 2\theta_1$ smaller (larger) than 0.82, and is thus disallowed (allowed). The additional line included has $\sin^2 2\theta_1 = 0.9$.

Finally, figure 4 presents contours of constant $\sin^2 2\theta_3$ which is relevant for oscillations of solar neutrinos. The grey (white) region has $\sin^2 2\theta_3$ larger (smaller) than 0.99. If one is willing to interpret the existing data as implying an upper bound of 0.99 on $\sin^2 2\theta_3$, then the grey region would be excluded. The plotted curve gives $\sin^2 2\theta_3 = 0.95$ ($\sin^2 2\theta_3 > 0.8$ in all the region shown).

The region of parameter space where all constraints on mixing angles and mass splittings are satisfied is given by the intersection of all white areas in figures 2 and 3. If $\sin^2 2\theta_3 < 0.99$ is imposed, then that intersection region, including now figure 4, is empty and no allowed region remains. It should be noticed that this fact does not come from an incompatibility between the previous constraint and the $\sin^2 2\theta_3 > 0.99$ obtained from neutrinoless double β -decay limits, eq. (10), in the $\theta_2 = 0$ approximation. If this were the case, it could be easily solved by decreasing the overall size of the neutrino masses, m_ν , in eq.(10), and this is not the case. Indeed, eq.(10) is satisfied in

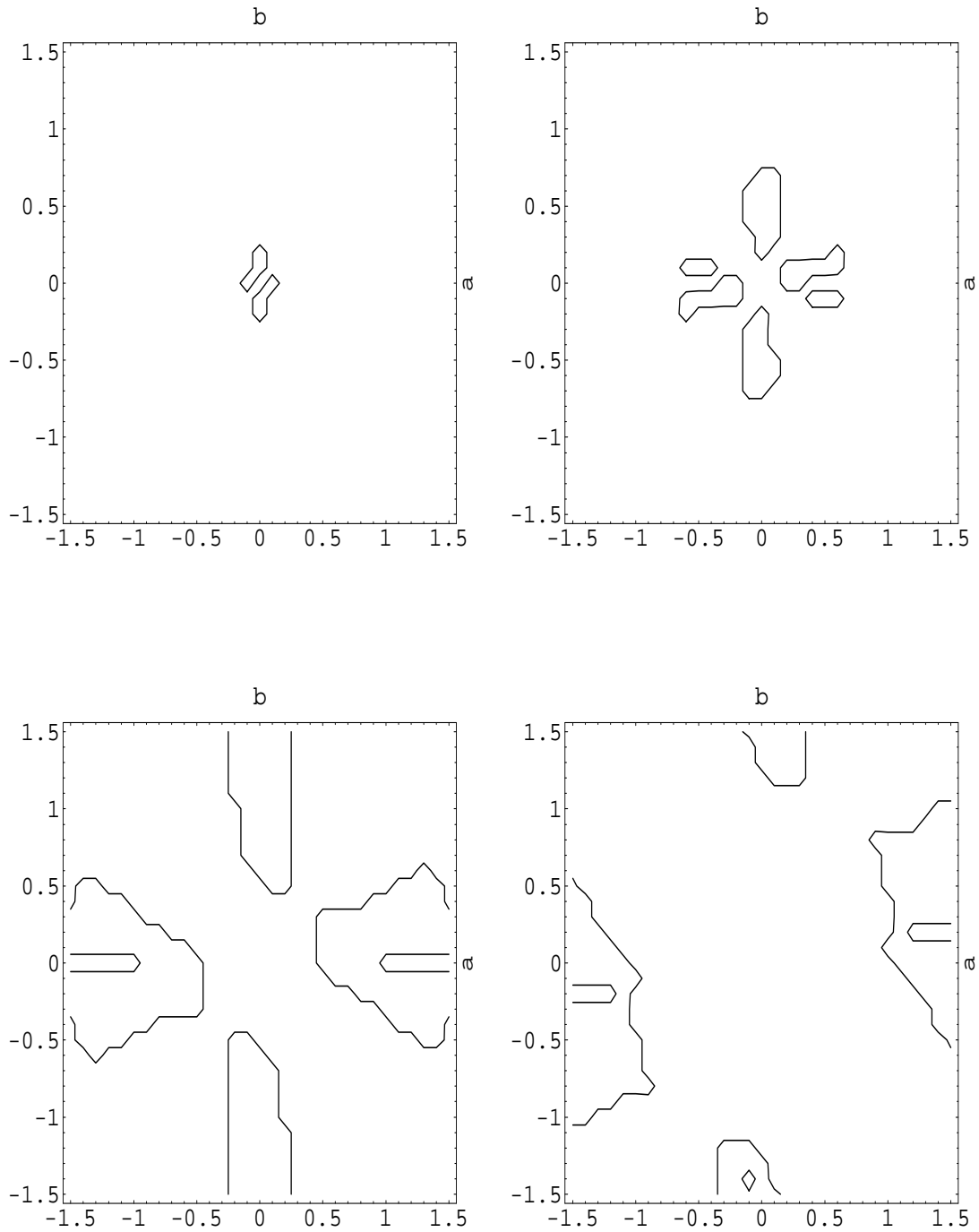


Figure 6:

Same as figure 5 for different values of the Majorana mass: Upper left: $M = 10^{12}$ GeV; Upper right: 10^{11} GeV; Lower left: 10^{10} GeV; Lower right: 10^9 GeV.

nearly all the parameter space. Even where $\sin^2 2\theta_3 < 0.99$ this is still true thanks to the contribution of θ_2 . What actually forbids the whole parameter space if $\sin^2 2\theta_3 < 0.99$ is imposed, is the incompatibility between acceptable θ_3 and θ_1 angles, as can be seen from the figures. This fact remains when m_ν is decreased. In fact, the effect of decreasing m_ν is essentially an amplification of the figures shown here, which comes from the fact that for a given Majorana mass, the neutrino Yukawa couplings become smaller.

If the $\sin^2 2\theta_3 > 0.99$ condition is relaxed (as discussed in the Introduction), then the allowed region is given by the four islands in figure 5, which is non-negligible.

If we now vary M , this allowed region will move in parameter space as indicated in figure 6, where we show the allowed regions for a sequence of Majorana masses that range from 10^9 to 10^{12} GeV. As is apparent from the figure, lowering M has the effect of enlarging the allowed region which flies away from the origin, leaving at some point the region of naturalness for a and b . At $M = 10^8$ GeV there is no allowed region inside the natural range for (a, b) . Conversely, increasing M reduces the allowed region, which gets closer to the origin. Let us remark again that in the allowed region one could fit the observed atmospheric and solar anomalies while part of the disallowed region corresponds in fact to the undecidable case (more precisely the region near the $a = b = 0$ origin), in which some additional physics could be invoked to explain the same data. In contrast, the region away from the origin becomes excluded. Let us also notice that if the $\sin^2 2\theta_3 > 0.99$ condition is imposed, the whole parameter space becomes excluded for any value of M .

We also find that, whenever there is a hierarchy in the mass splittings, the two lightest eigenvalues have opposite signs. This is just what is needed to have a cancellation occurring in the neutrinoless double β -decay constraint (10). This constraint is satisfied in almost the whole parameter space for any M .

This and other features of our results are discussed further in the next subsection.

3.5 Analytical understanding of results

It is simple and very illuminating to derive analytical approximations for the results presented in the previous subsection. The renormalization group equations (14,26,27,29) we integrated numerically can also be integrated analytically in the approximation of constant right hand side. In this approximation, the effective neutrino mass matrix at low-energy is simply \mathcal{M}_b plus some small perturbation. It is straightforward to obtain

how the degenerate eigenvalues of \mathcal{M}_b get split by this perturbation. Neglecting the Y_μ, Y_τ Yukawa couplings, we get the following analytical expressions:

$$\begin{aligned} m_{\nu_1} &\simeq m_\nu [-1 + (2c_a^2 c_b^2 - 1)\epsilon_\nu - 2\epsilon_\tau], \\ m_{\nu_{2,3}} &\simeq m_\nu \left[1 + 3\epsilon_\tau - c_a^2 c_b^2 \epsilon_\nu \pm \left\{ [\epsilon_\tau + (c_a^2 c_b^2 - c_{2a})\epsilon_\nu]^2 + [s_{2a} s_b \epsilon_\nu - 2\sqrt{2}\epsilon_\tau]^2 \right\}^{1/2} \right] \end{aligned} \quad (34)$$

where $c_a = \cosh a$, $s_{2a} = \sinh 2a$, etc, and

$$\epsilon_\tau = \frac{Y_\tau^2}{128\pi^2} \left[\log \frac{M}{M_Z} + 3 \log \frac{M_p}{M} \right], \quad (35)$$

$$\epsilon_\nu = \frac{Y_\nu^2}{16\pi^2} \log \frac{M_p}{M}. \quad (36)$$

It can be checked that, for $a = b = 0$, the \mathbf{Y}_ν couplings play no role in the mass splittings. This is not surprising since, as was mentioned in subsection 3.1, this case is equivalent to having all the structure in \mathcal{M} , while \mathbf{Y}_ν is proportional to the identity. Then, it can be seen from the RGEs that all the non-universal modifications on \mathcal{M}_ν come from the \mathbf{Y}_e matrix, and has a form similar to the one found in section 2 [see eq.(16)]. So this scenario gives similar (not satisfactory) results to those found in that section.

As $\epsilon_\nu \gg \epsilon_\tau$ (which occurs as soon as $Y_\nu > Y_\tau$, i.e for $M \gtrsim 10^9$ GeV), a further expansion in powers of $\epsilon_\tau/\epsilon_\nu$ of the square root is possible in most of the parameter space (except where the coefficient of ϵ_ν^2 inside that square-root becomes very small). The mass eigenvalues then read

$$\begin{aligned} m_{\nu_1} &\simeq m_\nu [-1 + (2c_a^2 c_b^2 - 1)\epsilon_\nu - 2\epsilon_\tau], \\ m_{\nu_2} &\simeq m_\nu \left[1 - (2c_a^2 c_b^2 - 1)\epsilon_\nu + \left(2 - \frac{1 - c_{2a} - 2s_{2a}s_b}{c_a^2 c_b^2 - 1} \right) \epsilon_\tau \right], \\ m_{\nu_3} &\simeq m_\nu \left[1 - \epsilon_\nu + \left(4 + \frac{1 - c_{2a} - 2s_{2a}s_b}{c_a^2 c_b^2 - 1} \right) \epsilon_\tau \right]. \end{aligned} \quad (37)$$

These expressions show clearly the origin of the neutrino mass splittings. The splitting between the first two neutrinos is controlled by the small parameter ϵ_τ , proportional to the squared Yukawa couplings of the charged leptons, and is insensitive to the parameter ϵ_ν (proportional to the square of the larger Yukawa coupling Y_ν) which is responsible for the mass difference of the third neutrino.

From the previous expressions we can extract the following remarkable conclusions. If the neutrino Yukawa couplings are sizable (i.e. bigger than Y_τ), we will automatically obtain a hierarchy of mass splittings $\Delta m_{12}^2 \ll \Delta m_{23}^2 \sim \Delta m_{13}^2$. This is exactly what is needed for a simultaneous solution of the atmospheric and solar neutrino anomalies, and thus represents a natural mechanism for the $\Delta m_{at}^2 \ll \Delta m_{sol}^2$ hierarchy. Thus, if the mixing angle θ_2 is small, as it turns out to be in most of the parameter space, Δm_{12}^2 is to be correctly identified with Δm_{sol}^2 and Δm_{23}^2 with Δm_{at}^2 . The two mass eigenvalues which are more degenerate correspond to the lighter states, i.e. $m_{\nu_1}^2 \sim m_{\nu_2}^2 < m_{\nu_3}^2$. Moreover, m_{ν_1} and m_{ν_2} have opposite signs in the diagonalized mass matrix, which is exactly what is needed to fulfill the neutrinoless double β -decay condition, eq.(10). All these nice features are illustrated in the explicit results presented in the previous subsection.

Concerning the mixing angles, it is straightforward to check that, working in the $Y_\nu > Y_\tau$ approximation, the eigenstates of the perturbed \mathcal{M}_ν matrix, corresponding to the previous eigenvalues, are

$$V'_1 = V_1, \quad V'_2 = \frac{1}{\sqrt{\alpha^2 + \beta^2}}(\alpha V_2 + \beta V_3), \quad V'_3 = \frac{1}{\sqrt{\alpha^2 + \beta^2}}(-\beta V_2 + \alpha V_3), \quad (38)$$

where V_i are the eigenstates corresponding to the bimaximal mixing matrix, V_b [see eq.(12)]

$$V_1 = \begin{pmatrix} \frac{-1}{\sqrt{2}} \\ \frac{1}{2} \\ \frac{1}{2} \end{pmatrix}, \quad V_2 = \begin{pmatrix} \frac{1}{\sqrt{2}} \\ \frac{1}{2} \\ \frac{1}{2} \end{pmatrix}, \quad V_3 = \begin{pmatrix} 0 \\ \frac{-1}{\sqrt{2}} \\ \frac{1}{\sqrt{2}} \end{pmatrix}, \quad (39)$$

and α, β are given by

$$\alpha = c_a s_b, \quad \beta = s_a. \quad (40)$$

The V'_i vectors define the new ‘‘CKM’’ matrix V' . Clearly, if just one of the two (a, b) parameters is vanishing, then $V' = V_b$, i.e. exactly the bimaximal mixing case. Also, whenever c_a, c_b are sizable (i.e. away from $a = b = 0$), $|\alpha| \gg |\beta|$, and thus we are close to the bimaximal case. Therefore, it is not surprising that in most of the parameter space shown in the previous section, this was in fact the case. This is remarkable, because it gives a natural origin for the bimaximal mixing, which was not guaranteed

a priori due to the ambiguity of the initial $\mathcal{M}_\nu(M_p) = \mathcal{M}_b$ matrix, as was explained in the Introduction.

3.6 Examples of acceptable ansatzs

In a generic point in the allowed regions we have found, the form of the matrix $\mathbf{Y}_\nu(M_p)$ would look rather ad-hoc: different elements in that matrix seem to conspire to give the correct neutrino mass texture. However, there are particular cases in which this matrix has a plausible structure. We give an example of such a texture for $\mathbf{Y}_\nu(M_p)$ which for the case $M \simeq 8 \times 10^9$ GeV studied in previous sections, would give mass splittings and mixing angles in agreement with observation:

$$\mathbf{Y}_\nu(M_p) = Y_\nu \begin{pmatrix} -\frac{1}{2\sqrt{2}} & 1 & 1 \\ \frac{1}{2\sqrt{2}} & 1 & 1 \\ 0 & -\frac{1}{\sqrt{2}} & \frac{1}{\sqrt{2}} \end{pmatrix}. \quad (41)$$

It corresponds to $a = 0$ and $b = -\sinh^{-1}(3/4) \simeq -0.69$, value which falls in the allowed region plotted in figure 5. More precisely, the mass splittings are

$$\Delta m_{12}^2 \simeq 2 \times 10^{-5} \text{ eV}^2, \quad \Delta m_{13}^2 \simeq 1 \times 10^{-3} \text{ eV}^2, \quad \Delta m_{23}^2 \simeq 1 \times 10^{-3} \text{ eV}^2, \quad (42)$$

and the mixing angles

$$\sin^2 \theta_2 = 0.04560, \quad \sin^2 \theta_1 = 0.95405, \quad \sin^2 \theta_3 = 0.99986. \quad (43)$$

It would be interesting to explore the possibility of finding a symmetry that could be responsible for the form of the matrix (41) and to analyze its implications for future long baseline experiments [17].

4 Conclusions

We have performed an exhaustive study of the possibility that radiative corrections are responsible for the small mass splittings in the (cosmologically relevant) scenario of nearly degenerate neutrinos. To do that, we assume that the initial form of the neutrino mass matrix (generated at high energy by unspecified interactions) has the bimaximal mixing form, and run down to low energy. We then examine the form of

the low-energy neutrino mass matrix, checking its consistency with all the available experimental data, including atmospheric and solar neutrino anomalies.

We find cases where the radiative corrections produce mass splittings that are *i*) just fine *ii*) too large or *iii*) too small. The vacuum oscillations solution to the solar neutrino problem always falls in the situation (*ii*), and it is therefore excluded. On the contrary, if the initial bimaximal mass matrix is produced by a see-saw mechanism (a possibility that we analyze in a detailed way), there are large regions of the parameter space consistent with the large angle MSW solution, providing a natural origin for the $\Delta m_{sol}^2 \ll \Delta m_{atm}^2$ hierarchy. Concerning the mixing angles, they are remarkably stable and close to the bimaximal mixing form (something that is not guaranteed a priori, due to an ambiguity in the diagonalization of the initial matrix).

We have explained analytically the origin of these remarkable features, giving explicit expressions for the mass splittings and the mixing angles. In addition, we have presented a particularly simple see-saw ansatz consistent with all the observations.

Finally, we have noted that the scenario is very sensitive to a possible upper bound on $\sin^2 2\theta_3$ (the angle responsible for the solar neutrino oscillations). An upper bound such as $\sin^2 2\theta_3 < 0.99$ would exclude completely the scenario of nearly degenerate neutrinos.

Addendum

Shortly after completion of this work, a paper by J. Ellis and S. Lola on the same subject appeared [18]. In it, the scenario of our section 2 is also studied and similar (negative) conclusions reached. However, as we show in our section 3, positive results are obtained when the general see-saw scenario as the mechanism responsible for the effective neutrino mass matrix is studied.

Also, the treatment by these authors of the constraints on mixing angles from neutrinoless double β -decay and LAMSW fits to solar neutrino data is more pessimistic than ours.

Acknowledgements

We thank D. Casper and E. Kearns for clarification of the results of Super-Kamiokande fits. This research was supported in part by the CICYT (contract AEN95-0195) and

the European Union (contract CHRX-CT92-0004) (JAC). J.R.E. thanks the I.E.M. (CSIC, Spain) and A.I, I.N the CERN Theory Division, for hospitality during the final stages of this work.

References

- [1] Y. Fukuda et al., Super-Kamiokande Collaboration, *Phys. Lett.* **B433** (1998) 9; *Phys. Rev. Lett.* **81** (1998) 1562; S. Hatakeyama et al., Kamiokande Collaboration, *Phys. Rev. Lett.* **81** (1998) 2016; M. Ambrosio et al., MACRO Collaboration, *Phys. Lett.* **B434** (1998) 451.
- [2] H. Georgi and S.L. Glashow, [hep-ph/9808293].
- [3] V. Barger, S. Pakvasa, T.J. Weiler and K. Whisnant, *Phys. Lett.* **B437** (1998) 107.
- [4] C. Giunti, *Phys. Rev.* **D59**:077301 (1999).
- [5] C.D. Carone and M. Sher, *Phys. Lett.* **B420** (1998) 83; A.S. Joshipura, *Z. Phys.* **C64** (1994) 31; A. Ioannisian and J.W.F. Valle, *Phys. Lett.* **B332** (1994) 93; D. Caldwell and R.N. Mohapatra, *Phys. Rev.* **D48** (1993) 3259; G.K. Leontaris, S. Lola, C. Scheich and J.D. Vergados, *Phys. Rev.* **D53** (1996) 6381; S. Lola and J.D. Vergados, *Prog. Part. Nucl. Phys.* **40** (98) 71; B.C. Allanach, [hep-ph/9806294]; A.J. Baltz, A.S. Goldhaber and M. Goldhaber, *Phys. Rev. Lett.* **81** (1998) 5730; R.N. Mohapatra and S. Nussinov, *Phys. Lett.* **B441** (1998) 299 and [hep-ph/9809415]; C. Jarlskog, M. Matsuda and S. Skadhauge, [hep-ph/9812282]; Y. Nomura and T. Yanagida, *Phys. Rev.* **D59**:017303 (1999); S.K. Kang and C.S. Kim, *Phys. Rev.* **D59**:091302 (1999); S. Davidson and S. King, *Phys. Lett.* **B445** (1998) 191; H. Fritzsch and Z. Xing, *Phys. Lett.* **B440** (1998) 313 and [hep-ph/9903499]; M. Tanimoto, *Phys. Rev.* **D59**:017304 (1998); N. Haba, *Phys. Rev.* **D59**:035011 (1999); Yue-Liang Wu, [hep-ph/9901245]; E. Ma, [hep-ph/9812344] and [hep-ph/9902465]; E.M. Lipmanov, [hep-ph/9901316]; T. Ohlsson and H. Snellman, [hep-ph/9903252]; A.H. Guth, L. Randall and M. Serna, [hep-ph/9903464].

- [6] R. Barbieri et al., *JHEP* **9812** (1998) 017; G.L. Fogli, E. Lisi, A. Marrone and G. Scioscia, *Phys. Rev.* **D59**:033001 (1998).
- [7] Y. Fukuda et al., Super-Kamiokande Collaboration, [hep-ex/9812009].
- [8] D. Casper and E. Kearns, private communication.
- [9] L. Baudis et al., Heidelberg-Moscow exp., [hep-ex/9902014].
- [10] V. Lobashev, Pontecorvo Prize lecture at the JINR, Dubna, January 1999; A.I. Belesenov et al., *Phys. Lett.* **B350** (1995) 263.
- [11] Y. L. Wu, [hep-ph/9810491], [hep-ph/9901245] and [hep-ph/9901320]; C. Wetterich, [hep-ph/9812426]; R. Barbieri, L.J. Hall, G.L. Kane, and G.G. Ross, [hep-ph/9901228].
- [12] G. Altarelli and F. Feruglio, *Phys. Lett.* **B439** (1998) 112, *JHEP* **9811** (1998) 021, and [hep-ph/9812475].
- [13] S. Weinberg, *Phys. Rev. Lett.* **43** (1979) 1566.
- [14] K. Babu, C. N. Leung and J. Pantaleone, *Phys. Lett.* **B319** (1993) 191.
- [15] M. Gell-Mann, P. Ramond and R. Slansky, proceedings of the Supergravity Stony Brook Workshop, New York, 1979, eds. P. Van Nieuwenhuizen and D. Freedman (North-Holland, Amsterdam); T. Yanagida, proceedings of the Workshop on Unified Theories and Baryon Number in the Universe, Tsukuba, Japan 1979 (edited by A. Sawada and A. Sugamoto, KEK Report No. 79-18, Tsukuba); R. Mohapatra and G. Senjanović, *Phys. Rev. Lett.* **44** (1980) 912, *Phys. Rev.* **D23** (1981) 165.
- [16] J.A. Casas, V. Di Clemente, A. Ibarra and M. Quirós, [hep-ph/9904295].
- [17] A. De Rújula, M.B. Gavela and P. Hernández, [hep-ph/9811390].
- [18] J. Ellis and S. Lola, [hep-ph/9904279].